

# Electrochemical CO<sub>2</sub> Capture by a Quinone-Based Covalent Organic Framework

Muhammad Abdullah Khan,\* Zhen Xu, Muhammad Muzammil, Samuel Bird, Monica Munawar, Fariah Salam, Niamh A. Hartley, Jack Taylor, Kamran Amin, Jianheng Ling, Henry R. N. B. Enniful, Naveed Zafar Ali, Kai Hetze, Sijia Cao, Yan Lu, Zhixiang Wei, Martin Oschatz, Phillip J. Milner, and Alexander C. Forse\*

Cite This: *J. Am. Chem. Soc.* 2025, 147, 47036–47043

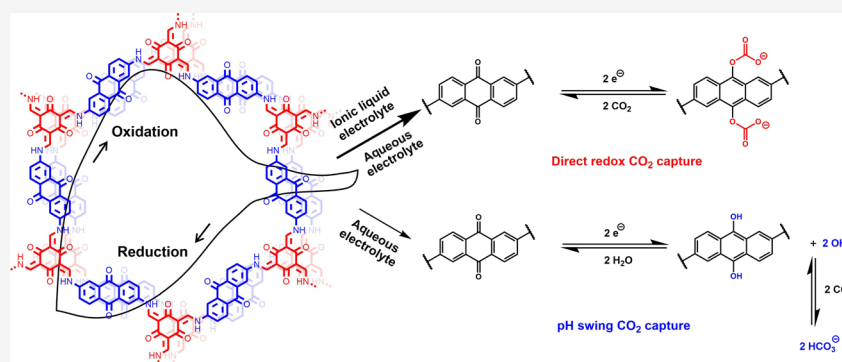
Read Online

ACCESS |

Metrics & More

Article Recommendations

Supporting Information



**ABSTRACT:** Electrochemical CO<sub>2</sub> capture is an emerging technology that promises to be more energy-efficient than traditional thermal or pressure-swing processes. Herein, the first evidence of electrochemical capture of CO<sub>2</sub> using a covalent organic framework (COF) is presented. We hypothesized that the assembly of anthraquinone units into a well-defined porous framework electrode would lead to enhanced electrochemical CO<sub>2</sub> capture compared to previous approaches that grafted anthraquinones on carbon supports and suffered from low CO<sub>2</sub> capacities and stabilities. To test this, an anthraquinone-based COF is employed, and it is found that the quinones are electrochemically accessible for reversible CO<sub>2</sub> capture in an ionic liquid electrolyte. The system achieves a high electrochemical CO<sub>2</sub> uptake capacity >2.6 mmol g<sup>-1</sup> COF, reaching half of the theoretical CO<sub>2</sub> capacity of the material and surpassing the capacities of anthraquinone-functionalized carbons. The stability and CO<sub>2</sub> uptake rate issues encountered with the ionic liquid system are also addressed by using aqueous electrolytes where we attained stable carbon capture for 500 cycles with a 99.6% Coulombic efficiency and an electrical energy consumption of 31 kJ mol<sub>CO<sub>2</sub></sub><sup>-1</sup>. The use of covalent organic framework electrodes can become a general strategy for understanding and enhancing the electrochemical CO<sub>2</sub> capture.

## INTRODUCTION

Energy-efficient CO<sub>2</sub> capture is vital for urgent climate change mitigation. As a promising alternative to traditional CO<sub>2</sub> capture methods, electrochemical CO<sub>2</sub> capture (eCC) employing switchable redox-active carriers is gaining significant momentum.<sup>1–5</sup> The research in this area is progressing in several directions including (i) the development of stable capture systems with higher CO<sub>2</sub> uptake capacities and (ii) the discovery of new solid sorbents that can operate at high current densities and are compatible with aqueous electrolytes.<sup>1,6–8</sup> On the first strand, by leveraging the redox behavior of active molecular disulfides, bipyridyls, thiolates, and extensively studied quinones, a diverse range of capture systems have been developed.<sup>9</sup> Even the simplest representatives of the quinone family have an appealingly high theoretical capacity of two CO<sub>2</sub> equivalents per molecule, compared to conventional

amines which require 2 equiv of amine to capture 1 equiv of CO<sub>2</sub>.<sup>1,2,6</sup> Importantly, eCC offers the benefit of conducting CO<sub>2</sub> capture and release without the need for external heating or heat removal and has thus shown promising energy efficiencies.<sup>2,10–12</sup>

Efforts to integrate solid CO<sub>2</sub> sorbents into eCC have seen remarkable initial successes. A notable example is the immobilization of polyanthraquinones on carbon nanotubes

Received: July 18, 2025  
Revised: November 15, 2025  
Accepted: November 23, 2025  
Published: December 9, 2025



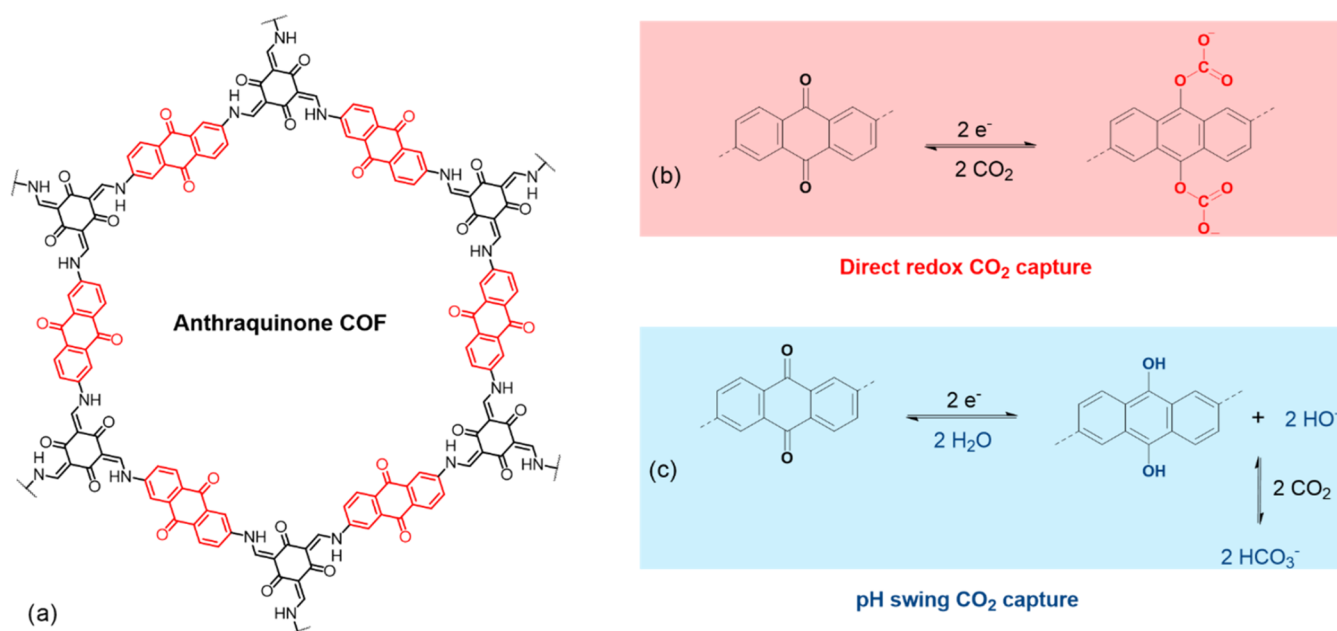


**Figure 1.** Proposed mechanisms of electrochemical CO<sub>2</sub> capture by an anthraquinone-based covalent organic framework. (a) Structure of the anthraquinone COF studied in this work. (b) “Direct redox” capture mechanism and (c) “pH swing” capture mechanism.

(CNTs) to build a semisolid faradaic swing system that demonstrated an impressive cyclic performance in both ionic liquid (IL) and water-in-salt electrolytes.<sup>13,14</sup> Building on this work, we successfully grafted anthraquinone (AQ) units onto conductive carbon substrates, achieving a 50% charge utilization of the loaded redox moieties for CO<sub>2</sub> capture. However, this system suffered from rapid CO<sub>2</sub> capacity loss over time, and it was challenging to control and characterize the quinone loading.<sup>15</sup> Furthermore, existing redox-based eCC systems often face challenges related to structural integrity, slow CO<sub>2</sub> uptake kinetics, and low mass loadings, imposing optimization and operational constraints.<sup>2,4,16,17</sup>

Motivated by the progress presented above, we hypothesized that the CO<sub>2</sub> affinity seen in molecular quinones could be replicated in quinone-based covalent organic framework (COF) materials. The electrochemical reduction of these materials would generate phenoxide anions, which could then bind electrophilic CO<sub>2</sub>, while the subsequent electrochemical oxidation would liberate CO<sub>2</sub> and regenerate the quinone (Figure 1). We propose that COF-based redox systems have a high density of well-defined active capture sites (the anthraquinone units), while the high COF porosity would enable the required rapid CO<sub>2</sub> and electrolyte transport. Additionally, the diversity of constituent redox moieties and COF structures offer possibilities to fine-tune the CO<sub>2</sub> uptake performance, while the use of earth-abundant C, N, H, and O elements is beneficial from a sustainability standpoint.<sup>18–20</sup> We note that one very recent study also explored a COF for electrochemical carbon dioxide capture, but ultimately did not observe any electrochemical capture by the phenazine framework which was explored, while it was also unclear to what extent the phenazine units were redox-active in the studied electrochemical cell.<sup>21</sup> The authors instead proposed the use of phenazine macrocycles as the redox-active capture materials, with these materials demonstrating accessible redox reactions, as well as electrochemically driven CO<sub>2</sub> capture and release.<sup>21</sup> Importantly, their study highlighted the key challenge of achieving good electron transport in covalent-

framework-type materials, which we have addressed further below.

## RESULTS AND DISCUSSION

To test the hypothesis in Figure 1, we synthesized a well-known anthraquinone-based COF (AQCOF) and employed it in electrochemical CO<sub>2</sub> capture experiments.<sup>22</sup> Details on the synthesis, characterization of the AQCOF, electrode preparation, and device assembly can be found in the Supporting Information (Sections S1–S4 and Figures S1–S6). In brief, our two-electrode battery-like cells are equipped with an AQCOF–carbon composite as the working electrode, an activated carbon counter electrode to balance the charge, 1-butyl-3-methylimidazolium bis(trifluoromethylsulfonyl)imide ionic liquid ([Bmim][TFSI], IL) as the electrolyte, and a pressure sensor to monitor electrochemical sorption and any irreversible pressure change associated with side reactions within the CO<sub>2</sub> environment of the cell.

When the cells were charged to negative voltages (i.e., by inducing the reduction of the AQCOF material), a CO<sub>2</sub> pressure drop was observed, supporting the electrochemical capture of CO<sub>2</sub> by the anthraquinone units (Figure 2a). A subsequent discharge back to 0 V led to a pressure increase ascribed to the electrochemical oxidation of the quinone units and CO<sub>2</sub> release. Importantly, the changes in the CO<sub>2</sub> pressure closely followed the applied cell voltage over repeated cycles, demonstrating that the cycle is reversible (Figure S7). From the observed pressure change, an initial uptake capacity of ~1.5 mmol g<sup>-1</sup> CO<sub>2</sub> uptake per gram of the AQCOF was calculated.

An improvement in the conductivity and charge capacity of the material was achieved by growing the AQCOF on carbon nanotubes (CNTs).<sup>23</sup> This addresses the limited accessibility of redox-active sites that often plagues COF–carbon composites.<sup>21</sup> To implement this in the device, the composition with 7% CNTs following AQCOF synthesis (denoted hereafter as AQCOF@CNTs) with a specific surface area (SSA) of 325 m<sup>2</sup> g<sup>-1</sup> was selected for its minimal surface

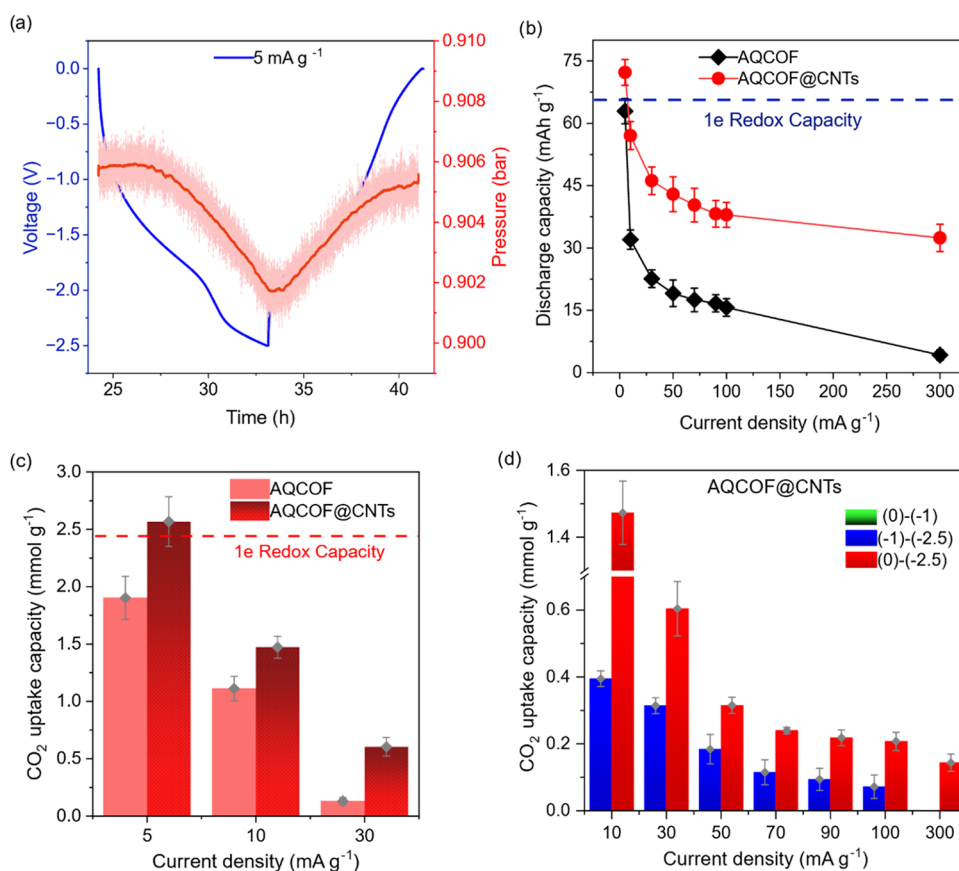


**Figure 2.** Electrochemical  $\text{CO}_2$  capture performance of AQCOF-based capture systems using [Bmim][TFSI] as the electrolyte. (a) A typical electrochemical galvanostatic discharge curve showing  $\text{CO}_2$  pressure changes (smoothed pressure curve, moving average every 100 s, red line) at a  $5 \text{ mA g}^{-1}$  constant current in static mode and with a 5 min voltage hold. (b) Electrochemical discharge capacities under  $\text{CO}_2$  at different current densities and (c)  $\text{CO}_2$  uptake capacities at low current densities, with data shown for electrodes made from the pristine AQCOF and electrodes made from AQCOF@CNT materials. (d) Effect of breaking the working voltage window into different voltage regimes on electrochemical  $\text{CO}_2$  uptake capacity using AQCOF@CNTs.

area difference with the pristine AQCOF ( $\text{SSA } 310 \text{ m}^2 \text{ g}^{-1}$ ). Electrodes fabricated with the AQCOF–carbon nanotube composite exhibited improved charge storage capacities compared to the AQCOF alone (Figure 2b) and attained  $1.09 \text{ e}^-$  ( $74 \text{ mAh g}^{-1}$  at  $5 \text{ mA g}^{-1}$ ) and  $\sim 0.85 \text{ e}^-$  ( $58 \text{ mAh g}^{-1}$  at  $10 \text{ mA g}^{-1}$ ) charge capacities per anthraquinone unit, indicating that quinone units remote from the conductive carbon additives might be electrically isolated and therefore not accessed.

Further insights into the electrochemical  $\text{CO}_2$  uptake performance were obtained by varying the current density during charge–discharge cycles (Figure 2c). In general, a high  $\text{CO}_2$  uptake is observed only at low current densities. Notably, at a current density of  $5 \text{ mA g}^{-1}$ , the  $\text{CO}_2$  uptake reached  $\sim 2.6 \text{ mmol g}^{-1}$  for AQCOF@CNTs. This  $\text{CO}_2$  uptake capacity is the best among all known capacitive or redox electrochemical capture systems where direct comparison is possible.<sup>8,15,21,24,25</sup> Fast charging shows a decreasing trend in both the  $\text{CO}_2$  uptake and the charge capacity, while right-shifted pressure curves portray a delayed  $\text{CO}_2$  uptake in response to the applied cell voltage (Figure S8a–c). This observation further supports our hypothesis of direct redox binding. The ideal electron-to- $\text{CO}_2$  ratio for system study is 1 (each anthraquinone unit can undergo two electron reductions, which can in principle capture two  $\text{CO}_2$  molecules). We found that the number of  $\text{CO}_2$  molecules captured per electron stored decreases

progressively and the electron/ $\text{CO}_2$  utilization ratio at 5, 10, and  $30 \text{ mA g}^{-1}$  for  $\text{CO}_2$  capture falls from 0.87 and 0.64 to  $0.34 \text{ e}^-$ , respectively (Figure S9), inferring that at higher current densities, the  $\text{CO}_2$  reaction in the COF channels and ion movement can no longer sustain the reaction rate and can limit the  $\text{CO}_2$  uptake in the cell.

The evidence of redox  $\text{CO}_2$  capture by the anthraquinone units was gathered with measurements in different voltage windows, along with cyclic voltammetry (CV) scans from two-electrode cells (Figure S10a,b). The CV of the AQCOF@CNTs under  $\text{CO}_2$  exhibits two distinct features (Figure S10b). Within the voltage range 0 to  $-1 \text{ V}$ , a narrow rectangular capacitive feature devoid of redox activity appears. Afterward, as the voltage was increased from  $-1$  to  $-2.25 \text{ V}$ , a broad peak became evident, assigned to anthraquinone reduction. This information combined with the galvanostatic charge–discharge profile presented in Figure 2a was then used to assess how voltage windows affect the  $\text{CO}_2$  uptake performance. As shown in Figure 2d, when the cell was operated within the purely capacitive range of 0 to  $-1 \text{ V}$ , no pressure change occurred (Figure S11a), suggesting that quinone redox is essential for driving electrochemical  $\text{CO}_2$  capture by the AQCOF. Instead, when limiting the voltage between  $-1$  and  $-2.5 \text{ V}$ , i.e., in a range of prominent redox activity, the  $\text{CO}_2$  pressure oscillated periodically in response to the applied voltage (Figure S11b). Nonetheless, the uptake remained lower than what was

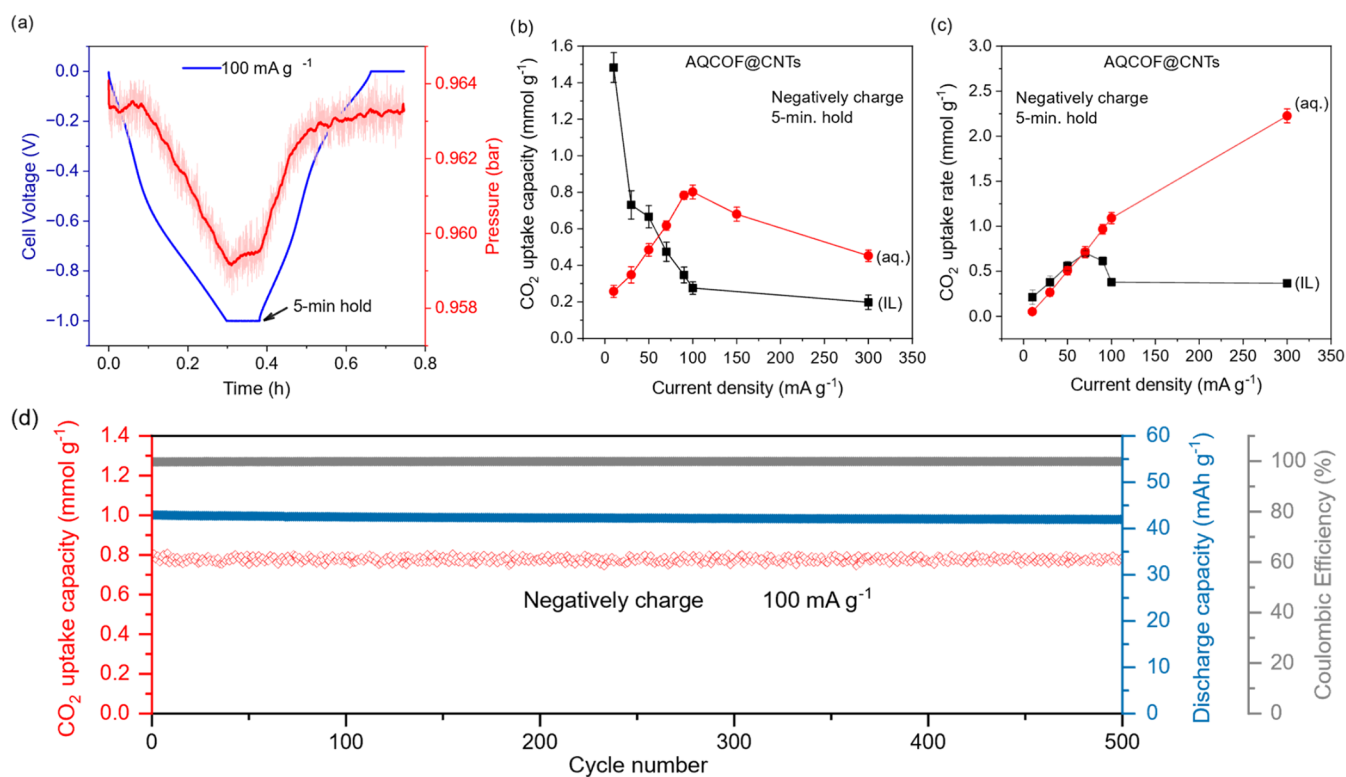


**Figure 3.** Electrochemical CO<sub>2</sub> capture performance of the AQCOF@CNT system in 1 M Na<sub>2</sub>SO<sub>4</sub> as the electrolyte. (a) CO<sub>2</sub> capture–release cycle recorded at a high current density of 100 mA g<sub>AQCOF@CNTs</sub><sup>−1</sup> (the shown data is a smoothed pressure curve moving average every 100 s, red) and a 5 min voltage hold. (b) Comparison of the discharge capacity under CO<sub>2</sub> and (c) CO<sub>2</sub> adsorption rate at different current densities measured in [Bmim][TFSI] and 1 M Na<sub>2</sub>SO<sub>4</sub> as the electrolyte. (d) Long cyclic stability in 1 M Na<sub>2</sub>SO<sub>4</sub> as the electrolyte. In all calculations, the net AQCOF@CNT mass in the electrode was used for the normalization.

recorded across the full 0 to −2.5 V range. Low CO<sub>2</sub> uptake at higher charging rates also indicated the need for more oxidizing potentials and more time to fully regenerate quinones to drive the next capture cycle. Furthermore, applying positive polarization from 0 to 2.5 V (i.e., positively charging the COF electrode) raised the pressure inside the cell with abrupt pressure changes, suggesting the degradation of the material (Figure S12). Subsequent operation of the cell within 0 to −2.5 V showed no pressure change, indicating that the cell was no longer functional. Our previous experiments with the electrochemical cell employing porous carbon electrodes as both electrodes and the same ionic liquid electrolyte exhibited only a very minor electrochemical CO<sub>2</sub> uptake,<sup>15</sup> supporting the idea that the CO<sub>2</sub> capture process by the AQCOF is predominantly driven by anthraquinone redox.

To assess our system under more realistic conditions, we evaluated the uptake capabilities in different gas mixtures. For 100% CO<sub>2</sub> and a 15% CO<sub>2</sub> mixture with N<sub>2</sub>, CO<sub>2</sub> uptake capacities were within error of each other (Figure S13a–d). To investigate whether the pressure changes were indeed due to CO<sub>2</sub> capture, measurements were conducted under 100% N<sub>2</sub> and showed only very small pressure changes (Figure S14). While small periodic pressure changes were observed under 100% N<sub>2</sub>, they remained the same in response to different current densities, and quantified values fell within the measurement uncertainty. We attribute these small changes to the movement of electrolyte ions within the COF channels and possible electrolyte density changes due to electrochemical charging. The O<sub>2</sub> sensitivity of anthraquinones is well documented.<sup>6,26,27</sup> Experiments under O<sub>2</sub>-containing atmos-

pheres (15% O<sub>2</sub>/20% CO<sub>2</sub>/60% N<sub>2</sub>; Figure S15a–d) show significant performance deterioration. We assumed the pressure changes come solely from CO<sub>2</sub> uptake (release), rather than N<sub>2</sub> uptake (release); CO<sub>2</sub> uptake decreased to 0.09 ± 0.02 mmol g<sup>−1</sup> at 100 mA g<sup>−1</sup> and 0.08 ± 0.03 mmol g<sup>−1</sup> at 50 mA g<sup>−1</sup>, respectively. Compared with Coulombic efficiencies under 100% CO<sub>2</sub> (97.6% at 100 mA g<sup>−1</sup> and 95.3% at 50 mA g<sup>−1</sup>), Coulombic efficiencies under oxygen at the same current densities dropped to 91.2 and 86.3%, respectively. The lower uptake at lower charging rates and the decreases in Coulombic efficiencies suggest that redox-active sites are reoxidized by oxygen, making them unavailable for CO<sub>2</sub> uptake, consistent with the known oxygen sensitivity of anthraquinone systems.<sup>6,26,27</sup> The observed O<sub>2</sub> sensitivity highlights an important design challenge for redox-active framework systems, and future optimization should extend studies to full flue-gas compositions, containing SO<sub>x</sub> and NO<sub>x</sub>. Finally, for stability evaluation, in long cycling experiments, the system was charged with an industry-relevant constant current of 100 mA g<sup>−1</sup>. A 20% loss in CO<sub>2</sub> capacity after 50 cycles and a 60% loss after 100 cycles were noted (Figure S16a–g). After 300 cycles, only 20% of the initial uptake capacity was retained. The system maintained a high Coulombic efficiency of 90% (Figure S17). Further limiting the voltage range between −1 and −2 V—a region of predominant redox activity—to minimize parasitic cell degradation at large voltages led to a lower CO<sub>2</sub> uptake but an improved capacity retention (~90%) after 100 cycles (Figure S18a–d). These stability issues in ionic liquids motivated us to explore alternate electrolytes.

Having identified key limitations of the capture process in the ionic liquid electrolyte, we replaced this electrolyte with an aqueous 1 M Na<sub>2</sub>SO<sub>4</sub> electrolyte. Recently, studies have begun to tackle the challenge of performing eCC with quinones in aqueous media.<sup>6,28,29</sup> Excitingly, a typical eCC cycle (Figure 3a) recorded using AQCOF@CNTs at 100 mA g<sup>-1</sup> in an aqueous cell exhibited a 4-fold increase in electrochemical CO<sub>2</sub> uptake compared to ionic liquid cells (IL ~0.2 mmol g<sup>-1</sup> and aq. ~0.8 mmol g<sup>-1</sup>), with the pressure curves closely following the applied voltage. The aqueous cell utilizes ca. 50% of the stored charge to capture CO<sub>2</sub> with an energy consumption of 37 kJ mol<sub>CO<sub>2</sub></sub><sup>-1</sup> at this current density, which is substantially lower than the binding enthalpy of traditional thermal amine processes.<sup>30,31</sup> Without a voltage hold under pure CO<sub>2</sub>, the uptake showed a negligible change (Figure S19a–c), but the electrical energy consumption of the capture process was further lowered to 31 kJ mol<sup>-1</sup> (Table S1).

Importantly, cyclic voltammetry studies confirmed the presence of quinone redox processes in the studied voltage range (Figure S20), and we further note that our observed electrochemical CO<sub>2</sub> uptake capacity of ~0.8 mmol g<sub>AQCOF@CNTs</sub><sup>-1</sup> is much larger than that observed in recently reported capacitive CO<sub>2</sub> capture processes,<sup>15,25,32,33</sup> indicating that quinone redox drives the electrochemical CO<sub>2</sub> capture process under aqueous conditions. In our previous work of a cell containing YP80F activated carbon as both the working and counter electrodes with the same aqueous electrolyte, we observed only ~0.1 mmol g<sup>-1</sup> CO<sub>2</sub> adsorption under identical conditions.<sup>24</sup> Moreover, when we positively charged the cell (0–1 V, i.e., oxidation of the AQCOF@CNT electrode), no CO<sub>2</sub> uptake was observed, further supporting that the reduction of quinones drives CO<sub>2</sub> capture (Figure S21).

Electrochemical CO<sub>2</sub> uptake capacities at different current densities displayed contrasting trends when compared to the ionic liquid system (Figures 3b and S22a–c). The ionic liquid system shows a gradual increase in uptake capacity as the applied current density is decreased, suggesting mass transport limitations at high currents. The aqueous system also shows an increase in the CO<sub>2</sub> capacity when the current density is decreased from 300 to 100 mA g<sup>-1</sup>; however, this is followed by decreases in capacity as the current density is reduced further (Figure 3b). This suggests that there may be competing mechanisms at play in the aqueous electrolyte, which are discussed further below.

To gauge the potential of the material for practical applications, uptake rates (i.e., CO<sub>2</sub> capture capacities per unit time) were determined. Figure 3c shows comparable adsorption rates for the IL and aqueous electrolyte systems until 70 mA g<sup>-1</sup>; beyond this point, rates improve further for the aqueous system. Similarly, improvements in Coulombic efficiencies were observed for both the IL and aqueous systems, rising from initial values of 83 and 95% at 5 mA g<sup>-1</sup> to 98 and 99.6% at 100 mA g<sup>-1</sup>, respectively, indicating a higher reversibility of electrochemical reactions in the aqueous system (Figure S23). The aqueous system also exhibited ultrahigh stability with no obvious charge storage or CO<sub>2</sub> capacity loss over 500 cycles and with a 99.6% Coulombic efficiency (Figure 3d). The cell is selective toward CO<sub>2</sub> in a mixture of 85% N<sub>2</sub>:15% CO<sub>2</sub>, (Figure S24), and in an optimized cycle (100 mA g<sup>-1</sup> charging current, no voltage holds, 0 to –0.8 V cell voltage window), an exceptionally low electrical energy consumption of 28 kJ mol<sup>-1</sup> and superior adsorption capacity

and adsorption rates were realized (Figure S25). However, measurements under 15% O<sub>2</sub> show only 0.34 mmol g<sup>-1</sup> CO<sub>2</sub> uptake with a decreased Coulombic efficiency of 91.2% (Figure S26a–d). Future work should address this challenge by developing redox-active COFs with more positive redox potentials and using stabilizing intermolecular interactions to break the unfavorable scaling relationship between the redox potential and the CO<sub>2</sub> binding energy.<sup>34</sup>

Postcycling analysis of COF@CNT electrode films shows structural changes after extended electrochemical use. In free-standing COF films, COF diffraction peaks are partially obscured by the polytetrafluoroethylene (PTFE) binder and CNTs, making it difficult to assess changes in crystallinity (Figure S27a–c). Films cycled in ionic liquid electrolytes show a reduced PTFE peak intensity, indicating a possible breakdown under high reductive currents. This degradation may cause decomposition products to accumulate within the porous structure and contribute to gradual capacity loss in the ionic liquid cell (Figures S16 and S17). Scanning electron microscopy (SEM) images of used electrodes reveal surface damage in the IL sample, and the comparatively aqueous sample largely remains morphologically stable (Figure S27d–f). These results indicate that the electrode films undergo mechanical degradation during extended cycling.

To try to better understand the underlying processes involved in the capture of CO<sub>2</sub> in aqueous cells, we explored different voltage regimes. While working in a 0 to –0.5 V window, a CO<sub>2</sub> uptake of ~0.2 mmol g<sup>-1</sup> was noted and was relatively constant at different current densities (Figure S28a). This behavior is similar to the trend seen in recent supercapacitive swing adsorption experiments.<sup>32,33</sup> In contrast, CO<sub>2</sub> uptake in the –0.5 to –1 V window showed a progressive increase as a function of current until 100 mA g<sup>-1</sup> where it reaches 0.4 mmol g<sup>-1</sup> (Figure S28b). We note the possibility of both the “direct redox capture” (Figure 1b) of CO<sub>2</sub> by the reduced anthraquinone units as well as the occurrence of pH swing (Figure 1c) in the aqueous electrolyte used here, which is discussed in more detail below.<sup>6,35</sup>

**CO<sub>2</sub> Capture Mechanism Study.** Evidence for direct redox capture (Figure 1b) by reduced AQCOF samples was obtained using a chemical reduction approach (SI Methods Section II, Figures S30–S42). In contrast to the parent AQCOF, the chemically reduced AQCOF exhibited pronounced CO<sub>2</sub> chemisorption in CO<sub>2</sub> adsorption isotherms and isobars (Figures S34 and S38). In the Fourier transform infrared (FTIR) spectra (Figures 4a and S35), the disappearance of the C=O stretch of the quinone following chemical reduction and the appearance of a new peak at ~1650 cm<sup>-1</sup> after CO<sub>2</sub> dosing are consistent with carbonate formation and closely match the spectral features reported for anthraquinone–CO<sub>2</sub> adducts in molecular systems.<sup>36,37</sup> These findings support the proposed mechanism of covalent CO<sub>2</sub> binding at the electrochemically reduced quinone sites. The CO<sub>2</sub> uptake behavior of COF@CNTs in an ionic liquid electrolyte under different voltage windows (Figures 2d and S11) also indicated that CO<sub>2</sub> uptake is initiated via quinone redox processes, consistent with the “direct capture” route to form anthraquinone–CO<sub>2</sub> adducts.

To assess the possible pH-driven CO<sub>2</sub> uptake in aqueous systems (Figure 1c), additional measurements were conducted in 0.1 and 0.5 M phosphate-buffered electrolytes, with all other conditions unchanged and a total ~2 M Na<sup>+</sup> concentration. These concentrations assume that all of the CO<sub>2</sub> uptake occurs

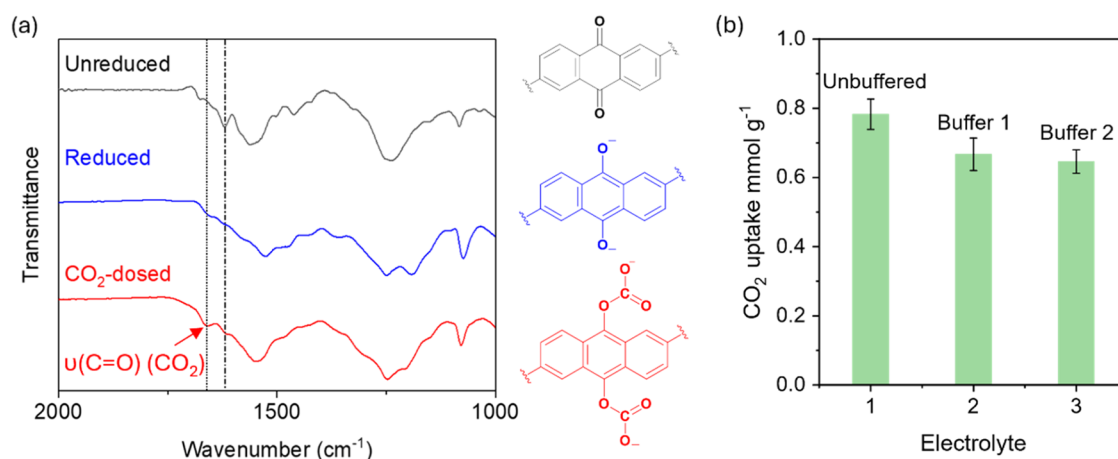


**Figure 4.** (a) FTIR spectra of the unreduced, chemically reduced, and CO<sub>2</sub>-dosed AQCOF material. (b) CO<sub>2</sub> uptake of AQCOF@CNTs in the unbuffered 1 M Na<sub>2</sub>SO<sub>4</sub> electrolyte and in phosphate-buffered electrolytes: Buffer 1 (0.1 M NaH<sub>2</sub>PO<sub>4</sub>/Na<sub>2</sub>HPO<sub>4</sub> with 0.9 M Na<sub>2</sub>SO<sub>4</sub>) and Buffer 2 (0.5 M NaH<sub>2</sub>PO<sub>4</sub>/Na<sub>2</sub>HPO<sub>4</sub> with 0.5 M Na<sub>2</sub>SO<sub>4</sub>).

via pH swing and exceeds those needed to suppress CO<sub>2</sub> uptake equilibria involving CO<sub>2</sub>, HCO<sub>3</sub><sup>-</sup>, and CO<sub>3</sub><sup>2-</sup> species. Results show a  $\sim(0.1-0.12) \pm 0.03$  mmol g<sup>-1</sup> decrease in CO<sub>2</sub> uptake under buffered conditions. This suggests that some of the apparent capacity in the unbuffered electrolyte comes from a surface-driven pH change, while most of the uptake is due to direct electrochemical capture by reduced quinone (Figures 4b and S29a–c). We tentatively propose that the pH swing mechanism might be responsible for the decrease in electrochemical CO<sub>2</sub> uptake seen at low current densities (Figure 3b) due to neutralization of pH changes by mass transport processes (e.g., H<sub>3</sub>O<sup>+</sup> diffusion) when charging slowly. Identification of the exact species involved and full clarification of the electrochemical CO<sub>2</sub> capture mechanisms in this system require further study.

## CONCLUSIONS

In conclusion, we have demonstrated the first example of the use of a covalent organic framework for electrochemical CO<sub>2</sub> capture. Electrochemical reduction of the anthraquinone units in the COF led to the electrochemical capture of CO<sub>2</sub> in electrochemical cells with both ionic liquid and aqueous electrolytes. While cells with ionic liquid electrolytes showed poor kinetic behavior and low stability, cells with aqueous electrolytes showed a greatly improved performance, with higher CO<sub>2</sub> uptake rates and excellent long-term stability. Our measurements also indicate a direct redox capture mechanism in ionic liquid electrolytes and both direct redox capture and pH swing mechanisms in aqueous electrolytes. Ultimately, this study opens a new material class for electrochemical CO<sub>2</sub> capture and may lead to further performance improvements as well as a new understanding of how to control the thermodynamics and kinetics of this important process. Future work should further explore the capture mechanism in these materials, and life cycle assessments and techno-economic analyses should be used to evaluate the sustainability and economics of the use of COFs for electrochemical separations.

## ASSOCIATED CONTENT

### Data Availability Statement

All data are available in the main text or in the [Supporting Information](#).

## Supporting Information

The Supporting Information is available free of charge at <https://pubs.acs.org/doi/10.1021/jacs.5c12304>.

Experimental details on synthesis; characterization of the materials; preparation of films, electrodes, and electrochemical cells; and details of the gas manifold and gas dosing setup, electrochemical gas cell device, CV measurements, electrochemical CO<sub>2</sub> capture measurements, and chemical reduction and CO<sub>2</sub> capture measurements (PDF)

## AUTHOR INFORMATION

### Corresponding Authors

**Muhammad Abdullah Khan** – Yusuf Hamied Department of Chemistry, University of Cambridge, Cambridge CB2 1EW, U.K.; Renewable Energy Advancement Laboratory, Department of Environmental Sciences, Quaid-i-Azam University, Islamabad 45320, Pakistan; Present Address: Institute for Technical Chemistry and Environmental Chemistry, Friedrich-Schiller-University, Philosophenweg 7a, 07743 Jena, Germany; [orcid.org/0000-0003-2500-8036](https://orcid.org/0000-0003-2500-8036); Email: [makhan@qau.edu.pk](mailto:makhan@qau.edu.pk)

**Alexander C. Forse** – Yusuf Hamied Department of Chemistry, University of Cambridge, Cambridge CB2 1EW, U.K.; [orcid.org/0000-0001-9592-9821](https://orcid.org/0000-0001-9592-9821); Email: [acf50@cam.ac.uk](mailto:acf50@cam.ac.uk)

### Authors

**Zhen Xu** – Yusuf Hamied Department of Chemistry, University of Cambridge, Cambridge CB2 1EW, U.K.; Department of Materials and Henry Royce Institute, University of Manchester, Manchester M13 9PL, U.K.; [orcid.org/0000-0001-9389-7993](https://orcid.org/0000-0001-9389-7993)

**Muhammad Muzammil** – Renewable Energy Advancement Laboratory, Department of Environmental Sciences, Quaid-i-Azam University, Islamabad 45320, Pakistan

**Samuel Bird** – Yusuf Hamied Department of Chemistry, University of Cambridge, Cambridge CB2 1EW, U.K.

**Monica Munawar** – Renewable Energy Advancement Laboratory, Department of Environmental Sciences, Quaid-i-Azam University, Islamabad 45320, Pakistan

- Fariah Salam** – Renewable Energy Advancement Laboratory, Department of Environmental Sciences, Quaid-i-Azam University, Islamabad 45320, Pakistan
- Niamh A. Hartley** – Yusuf Hamied Department of Chemistry, University of Cambridge, Cambridge CB2 1EW, U.K.
- Jack Taylor** – Yusuf Hamied Department of Chemistry, University of Cambridge, Cambridge CB2 1EW, U.K.
- Kamran Amin** – CAS Key Laboratory of Nanosystems and Hierarchical Fabrication, National Center for Nanoscience and Technology, Chinese Academy of Sciences, Beijing 100190, P. R. China; [orcid.org/0000-0001-7453-5305](https://orcid.org/0000-0001-7453-5305)
- Jianheng Ling** – Department of Chemistry and Chemical Biology, Cornell University, Ithaca, New York 14850, United States; [orcid.org/0000-0002-9821-2188](https://orcid.org/0000-0002-9821-2188)
- Henry R. N. B. Enniful** – Yusuf Hamied Department of Chemistry, University of Cambridge, Cambridge CB2 1EW, U.K.; Felix Bloch Institute for Solid State Physics, Faculty of Physics and Earth Sciences, Leipzig University, 504103 Leipzig, Germany
- Naveed Zafar Ali** – National Centre for Physics, Quaid-i-Azam University, Islamabad 44000, Pakistan
- Kai Hetze** – Institute for Technical Chemistry and Environmental Chemistry, Friedrich-Schiller-University Jena, 07743 Jena, Germany; Helmholtz Institute for Polymers in Energy Applications Jena, 07743 Jena, Germany
- Sijia Cao** – Institute of Electro chemical Energy Storage, Helmholtz-Zentrum Berlin für Materialien und Energie, 14109 Berlin, Germany; [orcid.org/0009-0001-2345-262X](https://orcid.org/0009-0001-2345-262X)
- Yan Lu** – Institute for Technical Chemistry and Environmental Chemistry, Friedrich-Schiller-University Jena, 07743 Jena, Germany; Helmholtz Institute for Polymers in Energy Applications Jena, 07743 Jena, Germany; Institute of Electro chemical Energy Storage, Helmholtz-Zentrum Berlin für Materialien und Energie, 14109 Berlin, Germany; [orcid.org/0000-0003-3055-0073](https://orcid.org/0000-0003-3055-0073)
- Zhixiang Wei** – CAS Key Laboratory of Nanosystems and Hierarchical Fabrication, National Center for Nanoscience and Technology, Chinese Academy of Sciences, Beijing 100190, P. R. China; [orcid.org/0000-0001-6188-3634](https://orcid.org/0000-0001-6188-3634)
- Martin Oschatz** – Institute for Technical Chemistry and Environmental Chemistry, Friedrich-Schiller-University Jena, 07743 Jena, Germany; Helmholtz Institute for Polymers in Energy Applications Jena, 07743 Jena, Germany; [orcid.org/0000-0003-2377-1214](https://orcid.org/0000-0003-2377-1214)
- Phillip J. Milner** – Department of Chemistry and Chemical Biology, Cornell University, Ithaca, New York 14850, United States; [orcid.org/0000-0002-2618-013X](https://orcid.org/0000-0002-2618-013X)

Complete contact information is available at:  
<https://pubs.acs.org/10.1021/jacs.5c12304>

## Notes

The authors declare no competing financial interest.

## ACKNOWLEDGMENTS

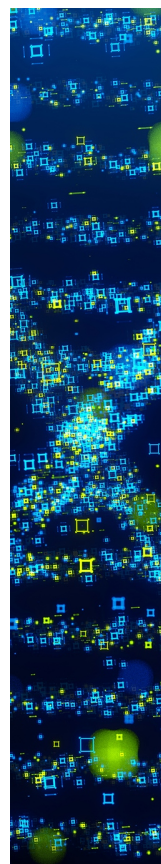
This work was supported by the Higher Education Commission (HEC) of Pakistan under NRPU Project 15273 awarded to M.A.K. M. Muzammil and M. Munawar acknowledge the HEC Pakistan for PhD studentships (NRPU 15273). A.C.F. acknowledges support from a UKRI Future Leaders Fellowship (MR/T043024/1). This work was also supported by the U.S. Department of Energy, Office of Science, Office of

Basic Energy Sciences under Award Numbers DE-SC0021000 and DE-SC0026238 (J.L., P.J.M.). P.J.M. further acknowledges support from a Camille Dreyfus Teacher-Scholar Award (TC-23-048). M.O. acknowledges financial support by the European Funds for Regional Development (Europäischer Fonds für Regionale Entwicklung; EFRE-OP 2021–2027; Project No. 2022 FGI 0007, DyNanoXRD). M.A.K. and M.O. acknowledge funding by the European Union (ERC, CILCat, project number 101040394). The views and opinions presented are solely those of the author(s) and do not necessarily represent those of the European Union or the European Research Council Executive Agency. The Union and the granting authority are not liable for any statements made. Authors thank Zeke Coody from Yusuf Hamied Department of Chemistry, Cambridge for helpful discussions and Dr. Z. Kochovski from HZB for the HR-TEM measurements.

## REFERENCES

- (1) Barlow, J. M.; Clarke, L. E.; Zhang, Z.; Bim, D.; Ripley, K. M.; Zito, A.; Brushett, F. R.; Alexandrova, A. N.; Yang, J. Y. Molecular Design of Redox Carriers for Electrochemical CO<sub>2</sub> Capture and Concentration. *Chem. Soc. Rev.* **2022**, *51* (20), 8415–8433.
- (2) Zito, A. M.; Clarke, L. E.; Barlow, J. M.; Bim, D.; Zhang, Z.; Ripley, K. M.; Li, C. J.; Kummeth, A.; Leonard, M. E.; Alexandrova, A. N.; Brushett, F. R.; Yang, J. Y. Electrochemical Carbon Dioxide Capture and Concentration. *Chem. Rev.* **2023**, *123* (13), 8069–8098.
- (3) Rheinhardt, J. H.; Singh, P.; Tarakeshwar, P.; Buttry, D. A. Electrochemical Capture and Release of Carbon Dioxide. *ACS Energy Lett.* **2017**, *2* (2), 454–461.
- (4) Renfrew, S. E.; Starr, D. E.; Strasser, P. Electrochemical Approaches toward CO<sub>2</sub> Capture and Concentration. *ACS Catal.* **2020**, *10* (21), 13058–13074.
- (5) Sharifian, R.; Wagterveld, R. M.; Digdaya, I. A.; Xiang, C.; Vermaas, D. A. Electrochemical Carbon Dioxide Capture to Close the Carbon Cycle. *Energy Environ. Sci.* **2021**, *14* (2), 781–814.
- (6) Jing, Y.; Amini, K.; Xi, D.; Jin, S.; Alfaraidi, A. M.; Kerr, E. F.; Gordon, R. G.; Aziz, M. J. Electrochemically Induced CO<sub>2</sub> Capture Enabled by Aqueous Quinone Flow Chemistry. *ACS Energy Lett.* **2024**, *9* (7), 3526–3535.
- (7) Namdari, M.; Kim, Y.; Pimlott, D. J. D.; Jewlal, A. M. L.; Berlinguette, C. P. Reactive Carbon Capture Using Electrochemical Reactors. *Chem. Soc. Rev.* **2025**, *54* (2), 590–600.
- (8) Liu, J.; Yang, M.; Zhou, X.; Meng, Z. Solid-State Electrochemical Carbon Dioxide Capture by Conductive Metal-Organic Framework Incorporating Nickel Bis(Diimine) Units. *J. Am. Chem. Soc.* **2024**, *146*, 33093.
- (9) Mizen, M. B.; Wrighton, M. S. Reductive Addition of CO<sub>2</sub> to 9,10-Phenanthrenequinone. *J. Electrochem. Soc.* **1989**, *136* (4), 941–946.
- (10) Forse, A. C.; Milner, P. J. New Chemistry for Enhanced Carbon Capture: Beyond Ammonium Carbamates. *Chem. Sci.* **2021**, *12* (2), 508–516.
- (11) Gurkan, B.; Simeon, F.; Hatton, T. A. Quinone Reduction in Ionic Liquids for Electrochemical CO<sub>2</sub> Separation. *ACS Sustainable Chem. Eng.* **2015**, *3* (7), 1394–1405.
- (12) Wang, Y.; Rogers, E. I.; Belding, S. R.; Compton, R. G. The Electrochemical Reduction of 1,4-Benzoquinone in 1-Ethyl-3-Methylimidazolium Bis(Trifluoromethane-Sulfonyl)-Imide, [C<sub>2</sub>mim][NTf<sub>2</sub>]: A Voltammetric Study of the Comproportionation between Benzoquinone and the Benzoquinone Dianion. *J. Electroanal. Chem.* **2010**, *648* (2), 134–142.
- (13) Liu, Y.; Ye, H. Z.; Diederichsen, K. M.; Van Voorhis, T.; Hatton, T. A. Electrochemically Mediated Carbon Dioxide Separation with Quinone Chemistry in Salt-Concentrated Aqueous Media. *Nat. Commun.* **2020**, *11* (1), No. 2278.

- (14) Voskian, S.; Hatton, T. A. Faradaic Electro-Swing Reactive Adsorption for CO<sub>2</sub> Capture. *Energy Environ. Sci.* **2019**, *12* (12), 3530–3547.
- (15) Hartley, N. A.; Pugh, S. M.; Xu, Z.; Leong, D. C. Y.; Jaffe, A.; Forse, A. C. Quinone-Functionalised Carbons as New Materials for Electrochemical Carbon Dioxide Capture. *J. Mater. Chem. A* **2023**, *11* (30), 16221–16232.
- (16) Rahimi, M.; Khurram, A.; Hatton, T. A.; Gallant, B. Electrochemical Carbon Capture Processes for Mitigation of CO<sub>2</sub> Emissions. *Chem. Soc. Rev.* **2022**, *51* (20), 8676–8695.
- (17) Diederichsen, K. M.; Sharifian, R.; Kang, J. S.; Liu, Y.; Kim, S.; Gallant, B. M.; Vermaas, D.; Hatton, T. A. Electrochemical Methods for Carbon Dioxide Separations. *Nat. Rev. Methods Primers* **2022**, *2* (1), No. 68.
- (18) Tan, K. T.; Ghosh, S.; Wang, Z.; Wen, F.; Rodríguez-San-Miguel, D.; Feng, J.; Huang, N.; Wang, W.; Zamora, F.; Feng, X.; Thomas, A.; Jiang, D. Covalent Organic Frameworks. *Nat. Rev. Methods Primers* **2023**, *3* (1), No. 1.
- (19) Zhou, Z.; Ma, T.; Zhang, H.; Chheda, S.; Li, H.; Wang, K.; Ehrling, S.; Giovine, R.; Li, C.; Alawadhi, A. H.; Abduljawad, M. M.; Alawad, M. O.; Gagliardi, L.; Sauer, J.; Yaghi, O. M. Carbon Dioxide Capture from Open Air Using Covalent Organic Frameworks. *Nature* **2024**, *635* (8037), 96–101.
- (20) Haldar, S.; Schneemann, A.; Kaskel, S. Covalent Organic Frameworks as Model Materials for Fundamental and Mechanistic Understanding of Organic Battery Design Principles. *J. Am. Chem. Soc.* **2023**, *145* (25), 13494–13513.
- (21) Le, P. H.; Liu, A.; Zasada, L. B.; Geary, J.; Kamin, A. A.; Rollins, D. S.; Nguyen, H. A.; Hill, A. M.; Liu, Y.; Xiao, D. J. Nitrogen-Rich Conjugated Macrocycles: Synthesis, Conductivity, and Application in Electrochemical CO<sub>2</sub> Capture. *Angew. Chem., Int. Ed.* **2025**, *64* (11), No. e202421822.
- (22) Amin, K.; Zhang, J.; Zhou, H. Y.; Lu, R.; Zhang, M.; Ashraf, N.; Yueli, C.; Mao, L.; Faul, C. F. J.; Wei, Z. Surface Controlled Pseudo-Capacitive Reactions Enabling Ultra-Fast Charging and Long-Life Organic Lithium Ion Batteries. *Sustainable Energy Fuels* **2020**, *4* (8), 4179–4185.
- (23) Duan, J.; Wang, W.; Zou, D.; Liu, J.; Li, N.; Weng, J.; Xu, L. P.; Guan, Y.; Zhang, Y.; Zhou, P. Construction of a Few-Layered COF@CNT Composite as an Ultrahigh Rate Cathode for Low-Cost K-Ion Batteries. *ACS Appl. Mater. Interfaces* **2022**, *14* (27), 31234–31244.
- (24) Xu, Z.; Mapstone, G.; Coady, Z.; Wang, M.; Spreng, T. L.; Liu, X.; Molino, D.; Forse, A. C. Enhancing Electrochemical Carbon Dioxide Capture with Supercapacitors. *Nat. Commun.* **2024**, *15* (1), No. 7851.
- (25) Bilal, M.; Li, J.; Landskron, K. Enhancing Supercapacitive Swing Adsorption of CO<sub>2</sub> with Advanced Activated Carbon Electrodes. *Adv. Sustainable Syst.* **2023**, *7* (11), No. 2300250.
- (26) Barlow, J. M.; Yang, J. Y. Oxygen-Stable Electrochemical CO<sub>2</sub> Capture and Concentration with Quinones Using Alcohol Additives. *J. Am. Chem. Soc.* **2022**, *144* (31), 14161–14169.
- (27) Abdinejad, M.; Massen-Hane, M.; Seo, H.; Hatton, T. A. Oxygen-Stable Electrochemical CO<sub>2</sub> Capture Using Redox-Active Heterocyclic Benzodithiophene Quinone. *Angew. Chem., Int. Ed.* **2024**, *63* (52), No. e202412229.
- (28) Huang, C.; Liu, C.; Wu, K.; Yue, H.; Tang, S.; Lu, H.; Liang, B. CO<sub>2</sub> Capture from Flue Gas Using an Electrochemically Reversible Hydroquinone/Quinone Solution. *Energy Fuels* **2019**, *33* (4), 3380–3389.
- (29) Abdinejad, M.; Reffet, M.; Tan, K.-J.; Hatton, T. A. Sustainable Electrochemical CO<sub>2</sub> Capture from Air Using Heterogenized Quinones in Aqueous Media. *ACS Sustainable Chem. Eng.* **2025**, *13*, 11425.
- (30) Khan, M. A.; Javed, A. H.; Qammar, M.; Hafeez, M.; Arshad, M.; Zafar, M. I.; Aldawsari, A. M.; Shah, A.; Rehman, Z. U.; Iqbal, N. Nitrogen-Rich Mesoporous Carbon for High Temperature Reversible CO<sub>2</sub> Capture. *J. CO<sub>2</sub> Util.* **2021**, *43*, No. 101375.
- (31) Siegel, R. E.; Pattanayak, S.; Berben, L. A. Reactive Capture of CO<sub>2</sub>: Opportunities and Challenges. *ACS Catal.* **2023**, *13* (1), 766–784.
- (32) Bilal, M.; Li, J.; Kumar, N.; Mosevitzky, B.; Wachs, I. E.; Landskron, K. Oxygen-Assisted Supercapacitive Swing Adsorption of Carbon Dioxide. *Angew. Chem.* **2024**, *136* (39), No. e202404881.
- (33) Xu, Z.; Liu, X.; Mapstone, G.; Coady, Z.; Seymour, C.; Wiesner, S. E.; Menkin, S.; Forse, A. C. Breaking Supercapacitor Symmetry Enhances Electrochemical Carbon Dioxide Capture. *J. Am. Chem. Soc.* **2025**, *147*, 16189–16197.
- (34) Li, X.; Zhao, X.; Zhang, L.; Mathur, A.; Xu, Y.; Fang, Z.; Gu, L.; Liu, Y.; Liu, Y. Redox-Tunable Isoindigos for Electrochemically Mediated Carbon Capture. *Nat. Commun.* **2024**, *15* (1), No. 1175.
- (35) Pang, S.; Jin, S.; Yang, F.; Alberts, M.; Li, L.; Xi, D.; Gordon, R. G.; Wang, P.; Aziz, M. J.; Ji, Y. A Phenazine-Based High-Capacity and High-Stability Electrochemical CO<sub>2</sub> Capture Cell with Coupled Electricity Storage. *Nat. Energy* **2023**, *8* (10), 1126–1136.
- (36) Li, H.; Zhou, Z.; Ma, T.; Wang, K.; Zhang, H.; Alawadhi, A. H.; Yaghi, O. M. Bonding of Polyethylenimine in Covalent Organic Frameworks for CO<sub>2</sub> Capture from Air. *J. Am. Chem. Soc.* **2024**, *146* (51), 35486–35492.
- (37) Diaye, J. N. ; Atifi, A. Electrochemically Mediated Carbon Capture on Surface-Confined Quinone: Unveiling Interfacial Pathways via Surface-Enhanced Spectroscopy. *ACS Electrochem.* **2025**, *1* (9), 1840–1851.



CAS BIOFINDER DISCOVERY PLATFORM™

## STOP DIGGING THROUGH DATA —START MAKING DISCOVERIES

CAS BioFinder helps you find the  
right biological insights in seconds

Start your search

**CAS**  
A Division of the  
American Chemical Society